ChemComm

Accepted Manuscript

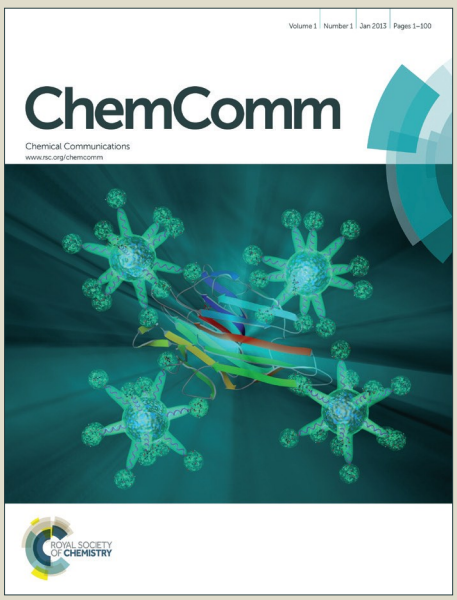

ROYAL SOCIETY OF CHEMISTRY

www.rsc.org/chemcomm

Journal Name

COMMUNICATION

Tumor Cell-Specific Split Aptamers: Target-Driven and Temperature-Controlled Self-Assembly on Living Cell Surface

Received 00th January 20xx,
Accepted 00th January 20xx

DOI: 10.1039/x0xx00000x

www.rsc.org/

Jinlu Tang,‡ Hui Shi,‡ Xiaoxiao He, Yanli Lei, Qiuping Guo, Kemin Wang,* Lv'an Yan, and Dinggeng He

Activatable split aptamer probe with target-induced shape change and thermosensitivity was first developed. Triggered by proteins on cell surface, the probe could assemble into a desired binding shape, thus affording a FRET-based tumor cell assay. Moreover, a reversible cell catch/release strategy was realized through mild temperature switching (4 °C/37 °C).

Target binding-induced conformational alteration is critical for molecular probes in monitoring and manipulating biological species in real time, *in situ* and *in vivo*.[1] Aptamers can bind to certain targets by folding into well-defined three-dimensional conformations.[2] The flexible shape change as well as high affinity, high specificity, easy synthesis and facile modification, make aptamers attractive as next-generation molecular tools for bioanalysis and biomedicine.[3] And with development of the cell-SELEX, which evolves aptamers against intact cells, the application of aptamers in cancer study has been promoted.[4] A variety of aptamers for various cancers, such as leukemia, lung cancer and so on, have been selected and used for cell detection, drug delivery and tumor marker discovery.[4b]

However, these tumor cell-specific aptamers are generally long oligonucleotides containing 30-100 bases.[3b,4b] Design of molecular probes using intact aptamers may pose limitations. First, efficiency and accuracy of synthesis will decrease with the increasing length of aptamers. Second, longer aptamers bear more secondary structures unfavorable for target binding, thus reducing effective probe concentration. Third, overlong sequences will increase challenges in designing activatable aptamer probes (AAPs) with target-induced large-scale shape alteration. For this reason, intact aptamers-based methods are still widely used in current cancer study, although they need time-consuming washing and lack real-time responses.[5] In recent years, our group has made a great effort to develop AAPs for theranostics.[6] Several competitive binding-based AAPs were designed and applied in cancer imaging inside mice.[6b,6f] Nevertheless, these AAPs still have problems ... much longer sequences than original aptamers, as well as fals positive and background elevation due to undesired stimul such as nuclease degradation. Hence, there is an urgent nee for novel concepts to design AAPs with both short sequenc and tumor cell-specific conformational activation.

Split aptamers consist of two fragments derived from pare t aptamers.[7] In the free state, the two strands are independent and nonfunctional. Once encountering targets, split ones ca assemble to a desired binding conformation.[8] Compared with intact aptamers, split ones are much shorter, thus showing merits of lower synthesis cost, less ineffective structures and simpler design for AAPs.[9] Also, different from competitive binding-based strategies, the shape change of split ones could just be induced by targets, suggesting a good anti-interferenc performance. But in contrast to hundreds of intact aptamer only several split ones have been developed and their targets focus on small molecules and biomolecules, such as cocaine thrombin, and so on.[10] Split aptamers for complex an dynamic targets like living cells have rarely been reported.

Herein, we present a rational and smart example of tumor cell-specific split aptamers being engineered and applied, b using Sgc8 aptamer against leukemia CCRF-CEM cells[11] as main model. Sgc8 was evolved by cell-SELEX and identified t interact with a cancer-associated membrane protein tyrosin kinase-7 (PTK-7).[12] To simplify sequence screening, Sgc8c truncated version of Sgc8[13]) was finally adopted to design split strategies. As shown in **Figure 1A**, the secondary structur of Sgc8c was roughly a stem-loop hairpin shape. Due to bases No. 23-30 (5'-3') in the loop region were not essential for targ binding,[13] cleavage sites were selected among these 8 base Three split ways were then designed, generating 6 fragment and 9 pairs of split aptamers. And their binding ability to targe cells was inspected using flow cytometry with Cy5-labeled b

State Key Laboratory of Chemo/Biosensing and Chemometrics, College of Chemistry and Chemical Engineering, College of Biology, Hunan University, Key Laboratory for Bio-Nanotechnology and Molecular Engineering of Hunan Province, Changsha, 410082, China. E-mail: kmwang@hnu.edu.cn.
‡J.L. Tang and H. Shi contributed equally to this work.
Electronic Supplementary Information (ESI) available: See
DOI: 10.1039/x0xx00000x

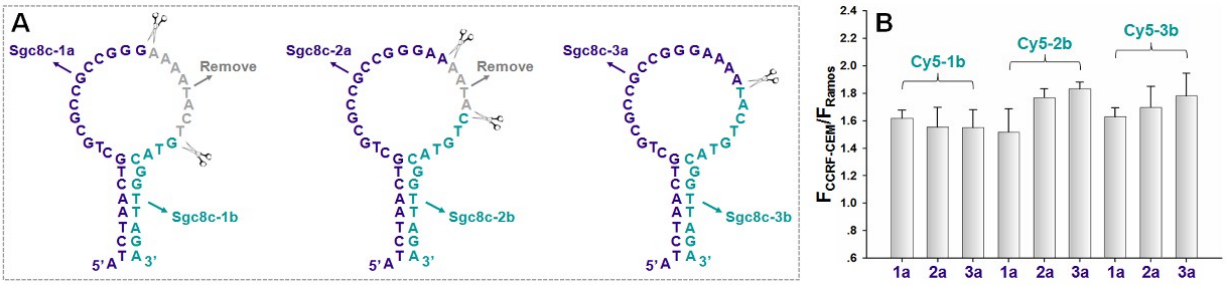

Figure 1. Screening of tumor cell-specific split aptamers. (A) Design of split strategies for Sgc8c, generating 6 DNA fragments and 9 pairs of split aptamers. (B) Histogram of the fluorescence ratios of CCRF-CEM to Ramos cells ($F_{CCRF-CEM}/F_{Ramos}$) after incubation with 9 pairs of split aptamers respectively. The fluorescence was detected using flow cytometry. (Incubation: on ice and 60 min. Concentration: 25 nM for a strands and 200 nM for Cy5-b strands. Error bars: standard deviations from three repeated experiments.)

(**Figure S1**, **Figure 1B**). It was revealed that sequence completeness had an obvious effect on binding. The removal of 4 or more bases led to a loss of affinity. But two bases "TA" (*Nos.* 27, 28) were dispensable, thus affording an optimal cleavage site and a pair of split Sgc8c (Sgc8c-3a/Sgc8c-2b). Then, a comparison of split ones (Sgc8c-3a/Cy5-Sgc8c-2b) with the parent aptamer (Cy5-Sgc8c) was performed. As displayed in **Figure 2A**, at the temperature for Sgc8 evolving (on ice), the split Sgc8c exhibited a much higher fluorescence response to target CCRF-CEM cells than control probe Cy5-Sgc8c-2b. And the fluorescence intensity from split Sgc8c was equivalent to that from Cy5-Sgc8c, suggesting split ones might assemble into an aptamer-target complex to afford a similar affinity as its parent. But considering that intact Sgc8c could achieve a good binding to target cells after incubation for less than 45 min[6f], and split Sgc8c need a 90 min-incubation for stable binding, we speculated that affinity of split aptamers might be slightly weaker than intact ones. Interestingly, a temperature dependent binding was measured for split Sgc8c. With increase of temperature, the signal of CCRF-CEM cells labeled by split Sgc8c gradually decreased. Especially at 37 °C, split Sgc8c nearly totally lost its recognition activity, showing same fluorescence response as control. This was different from its parent, which could hold a good binding at up to 42 °C.[14] And considering that 37 °C wouldn't negatively affect cell viability and target proteins, we guessed the failure in recognition might be due to inactivity of split Sgc8c itself. It was split design that introduced a novel thermosensitivity into tumor cell-specific aptamers. Specificity was also investigated using Ramos cells as control. Split Sgc8c always showed much lower nonspecific responses than Cy5-Sgc8c, and held a much higher signal-to-background ratio at the optimal temperature (**Figure 2B**, **Figure S2**). We deduced that the much shorter sequence of split ones might reduce secondary structures and weaken nonspecific binding. Thereupon, a novel split Sgc8 probe against CCRF-CEM cells was developed with good affinity and specificity as well as temperature-sensitivity.

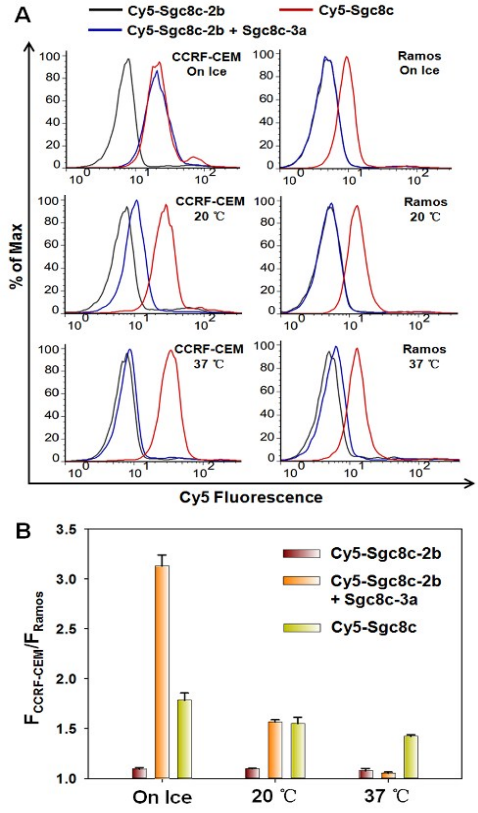

Figure 2. Comparison of the split aptamer (Sgc8c-3a/Cy5-Sgc8c-2b) with the parent aptamer (Cy5-Sgc8c). (A) Flow cytometry assays of CCRF-CEM or Ramos cells after a 90-min incubation with different probes at different temperatures. (Sgc8c-3a: 320 nM; Cy5-Sgc8c-2b: 40 nM; Cy5-Sgc8c: 40 nM.) (B) The corresponding histogram of the fluorescence ratios of CCRF-CEM to Ramos cells ($F_{CCRF-CEM}/F_{Ramos}$). (Error bars: standard deviations from three repeated experiments.)

We next illuminated the assembly behavior of split Sgc8c on target cell surface using a FRET-based AAP strategy. As seen in **Figure 3**, Sgc8c-3a was labeled by Cy3 at the 3'-terminal (Sgc8c-3a-Cy3) and Sgc8c-2b was labeled by Cy5 at the 5'-terminal (Cy5-Sgc8c-2b). It was envisaged that a target-driven self-assembly of Sgc8c-3a-Cy3 and Cy5-Sgc8c-2b on cell surface could keep Cy3 in close proximity to Cy5, thus leading to an activated FRET signal. To verify this assumption, CCRF-CEM cells after incubation with different probes were tested with flow cytometry at FL2 (Cy3 channel), FL3 (Cy3-Cy5 FRET channel) and FL4 (Cy5 channel) respectively. Sgc8c-3a-Cy3-treated cells (**group 1**) showed faint signal at both FL2 and FL3. After added with Sgc8c-2b, the signal at FL2 was enhanced due to interaction of split Sgc8c and target cells, but the signal at FL3 did not change obviously (**group 2**). When Sgc8c-2b was substituted by Cy5-Sgc8c-2b (**group 3**), an obvious signal decrease at FL2 and a great signal increase at FL3 were both observed, indicating an activated FRET. By analyzing the signal variation of **groups 3-5**, a same conclusion was gotten

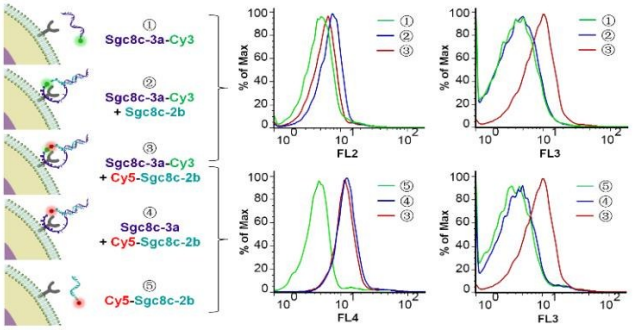

Figure 3. Schematic illustration and flow cytometry investigation of the target-driven assembly of split aptamers on cell surface based on FRET using Cy3-Cy5 as the donor-acceptor pair. CCRF-CEM cells were incubated with different probes on ice for 90 min and then measured at different channels. [FL2 (Cy3): 488 nm excitation and 564-606 nm emission; FL3 (FRET): 488 nm excitation and 670 nm long pass emission; FL4 (Cy5): 633 nm excitation and 653-669 nm emission. DNA concentration: 25 nM 3a/200 nM 2b.]

revealing that the enhanced signal at FL3 was not due to simple adsorption or binding of Cy5-Sgc8c-2b to cells. It was believed that in presence of target cells, two independent and nonfunctional split fragments could be induced by cell surface proteins to assemble into a desired binding shape similar to the intact aptamer. Also, the target-driven assembly of FRET-based split Sgc8c on living cell surface was testified to be selective (**Figure 4**), which strongly supported an effective and activatable assay for tumor cells. Subsequently, the effect of several factors on assembly of split Sgc8c was tested (**Figure S3**). It was found that FRET signals were dependent upon the ratio and concentration of two strands as well as incubation time of probes and cells. In addition, a temperature-controlled reversible assembly of split Sgc8c on CCRF-CEM cell surface was detected (**Figure S4**). This promises a great potential of applications in controllable manipulation of tumor cells.

We then investigated the split aptamer-assisted assembly of tumor cells on microwell surface. The avidin-coated 96-well microplate was modified with Biotin-T_{10}-Sgc8c-3a (**Figure 5A**). In presence of Sgc8c-2b, target cells could be captured on well surface after a simple incubation on ice due to target-driven assembly of split aptamers. Once temperature was adjusted to 37 °C, pre-captured cells would be released into supernatants. After optimizing the modification concentration of Biotin-T_{10}-Sgc8c-3a (**Figure S5**), a series of experiments were conducted to confirm the above idea. As displayed in **Figure 5B**, cells were only captured in Sgc8c-3a-coated wells incubated with both CCRF-CEM cells and Sgc8c-2b (**group d**), showing a density of

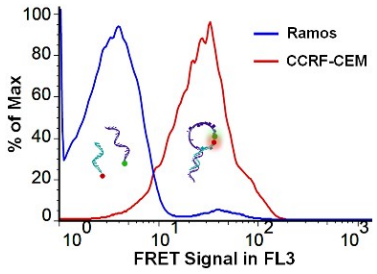

Figure 4. Selective detection of CCRF-CEM cells using a FRET-based AAP strategy. Flow cytometry assays of cells after incubation with Sgc8c-3a-Cy3/Cy5-Sgc8c-2b (25 nM/200 nM) on ice in the dark for 90 min.

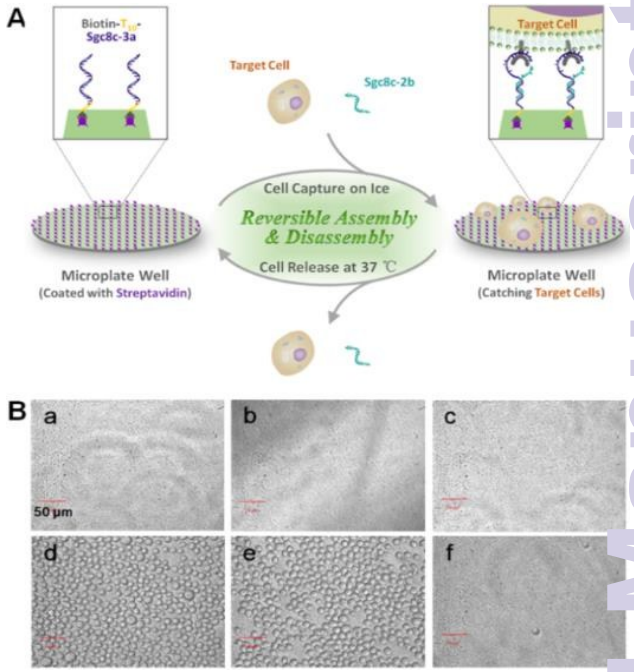

Figure 5. Temperature-controlled reversible assembly and disassembly of target cells on microplate well surface assisted by split aptamers. (A) Schematic illustration of the principle. (B) Feasibility investigation. (a-f: bright-field images. a: capture of CCRF-CEM cells in a blank well added with Sgc8c-2b; b: capture of CCRF-CEM cells in a Sgc8c-3a-coated well; c: capture of Ramos cells in a Sgc8c-3a-coated well added with Sgc8c-2b; d: capture of CCRF-CEM cells in a Sgc8c-3a-coated well added with Sgc8c-2b; e: release of d after incubation on ice for 1 h, f: release of d after incubation at 37 °C for 1 h.)

4638±394 cells/mm^2 (**Figure S6**). In other control **groups (a-c)**, few cells were observed. Next, the feasibility of temperature-controlled cell release was testified by incubating pre-captured cells for 1 h on ice and at 37 °C, respectively. It was shown that pre-captured cells were not released on ice (**group e**), in which case a density of 4200±551 cells/mm^2 was observed. In contrast, incubation at 37 °C effectively released pre-captured cells by destroying split Sgc8c-target ensembles (**group f**), thus inducing a sharp fall of cell density to 18±6 cells/mm^2. Combined with the temperature switch, split aptamer could control assembly and disassembly of tumor cells on microwell surface. Then, influence of the capture/release process on cell viability was inspected (**Figure S7**), which confirmed that this strategy not only was mild and biocompatible, but also could remove dead cells. Also, the recycling performance of Sgc8c-3a-coated wells for reversible cell manipulation was testified (**Figure S8**), which showed that the mild temperature switch did not harm well surface coating and supported a circular use.

Finally, we explored generality of the split aptamer-based strategy for temperature-controlled manipulation of tumor cells. Another pair of split aptamer (ZY11a and ZY11b) derived from the parent aptamer ZY11, which was selected against human hepatocellular cancer SMMC-7721 cells through cell-SELEX in our group, was used. Flow cytometry assays revealed a thermosensitive binding activity of split ZY11 (**Figure S9**). Then, the two pairs of split aptamers were applied to collect respective target cells from mixed cell samples by using the temperature-controlled cell assembly strategy. As presented in **Figure 6**, before a capture process, both green CCRF-CEM cells

and blue SMMC-7721 cells were observed. After incubation on ice in a Sgc8c-3a-coated well with Sgc8c-2b and a ZY11b-coated well with ZY11a respectively, green cells and blue cells were absolutely separated. Next, by adjusting temperature to 37 °C, cell release was realized. Accordingly, CCRF-CEM and SMMC-7721 cells were collected in respective supernatants. The successful separation and harvest of different cells in mixed samples was thus demonstrated, which again supported the effectiveness and specificity of split aptamers.

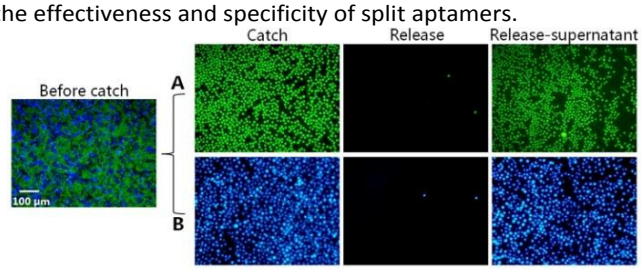

Figure 6. Selective capture and separation of mixed cell samples. The calcein-AM-labeled CCRF-CEM cells (green) and the Hoechst-33342-labeled SMMC-7721 cells (blue) were mixed with a ratio of 1:1. Fluorescence images were recorded before or after capture/release treatments using (A) Sgc8c-3a-coated wells added with Sgc8c-2b, or (B) ZY11b-coated wells added with ZY11a. (Each image is the merged one of green and blue fluorescence.)

In summary, a novel tumor cell-specific split aptamer probe composing of two strands with <30 bases was generated from an intact sequence with >80 bases. Compared with its parent, split aptamer held a similar target binding, less nonspecific adsorption and an additional thermosensitivity. By using a Cy3-Cy5 FRET strategy, target-driven self-assembly of split ones into desired binding shape on cell surface was demonstrated. The large-scale shape change facilitates exploring AAPs to detect tumor cells. Assisted by split aptamers, temperature-controlled reversible assembly of target cells on microwell surface was realized. In view of the significance of tumor cell catch/release study,[15] such a mild, biocompatible and reusable strategy is expected to be integrated in microfluidic chips to develop novel devices for circular tumor cell researches. It is also believed that the split strategy might be applicable to not only hairpin shape but also other aptamer structures, such as V-shape (**Figure S10**) and three-way junction architectures[16].

This work was supported by the National Natural Science Foundation of China (Grants 21190044, 21221003, 21322509, 21305035 and 21305038), and the Hunan Provincial Natural Science Foundation (Grant 2015JJ3044).

Notes and references

1 (a) A. Vallée-Bélisle, F. Ricci and K. W. Plaxco, *Proc. Natl. Acad. Sci. USA*, 2009, **106**, 13802-13807. (b) S. Tyagi and F. R. Kramer, *Nat. Biotech.*, 1996, **14**, 303-308. (c) Z. Tang, P. Mallikaratchy, R. Yang, Y. Kim, Z. Zhu, H. Wang and W. Tan, *J. Am. Chem. Soc.*, 2008, **130**, 11268-11269.

2 (a) C. Tuerk and L. Gold, Science, 1990, **249**, 505-510. (b) S. D. Jhaveri, R. Kirby, R. Conrad, E. J. Maglott, M. Bowser, R. T. Kennedy, G. Glick and A. D.Ellington, *J. Am. Chem. Soc.*, 2000, **122**, 2469-2473. (c) C. J. Yang, S. Jockusch, M. Vicens, N. J. Turro and W. Tan, *Proc. Natl. Acad. Sci. USA*, 2005, **102**, 17278-17283.

3 (a) Y. Du, B. Li and E. Wang, *Acc. Chem. Res*. 2013, **46**, 2[illegible] 213. (b) X. Fang and W. Tan, *Acc. Chem. Res*. 2010, **43**, 48-57 (c) T. T. Chen, X. Tian, C.-L. Liu, J. Ge, X. Chu and Y. Li, *J. Am. Chem. Soc*., 2015, **137**, 982-989.

4 (a) K. Sefah, D.Shangguan, X. Xiong, M. B. O'Donoghue [illegible] Tan, W. *Nat. Protoc.*, 2010, **5**, 1169-1185. (b) W. Tan, M. [illegible] Donovan and J. Jiang, *Chem. Rev.*, 2013, **113**, 2842-2862.

5 (a) J. Li, J. You, Y. Dai, M.Shi, C.Han and K. Xu, *Anal. Chem.*, 2014, **86**, 11306-11311. (b) Y. Wu, K. Sefah, H. Liu, R. Wang and W. Tan, *Proc. Natl. Acad. Sci. USA*, 2010, **107**, 5-10. (c) S. Wang, H. Kong, X. Gong, S. Zhang and X. Zhang, *Anal. Chem.*, 2014, **86**, 8261-8266. (d) C. Zhang, X. Ji, Y. Zhang, G. Zhou, X. Ke, H. Wang, P. Tinnefeld and Z. He, *Anal. Chem.*, 2013, **85**, 5843-5849.

6 (a) L. Yan, H. Shi, X. He, K. Wang, J. Tang, M. Chen, X. Ye, F. Xu and Y. Lei, *Anal. Chem.*, 2014, **86**, 9271-9277. (b) H. Shi, [illegible] Ye, X. He, K. Wang, W. Cui, D. He, D. Li and X. Jia, *Nanoscale*, 2014, **6**, 8754-8761. (c) H. Shi, D. Li, F. Xu, X. He, K. Wang, [illegible] Ye, J. Tang and C. He, *Analyst*, 2014, **139**, 4181-4184. (d) Huang, X.Yang, X. He, K. Wang, J. Liu, H. Shi, Q. Wang, Q.Guo and D. He, *TrAC-Trend.*, 2014, **53**, 11-20. (e) J. Yin, X. He, [illegible] Wang, F. Xu, J. Shangguan, D. He and H. Shi, *Anal. Chem.*, 2013, **85**, 12011-12019. (f) H. Shi, X. He, K. Wang, X. Wu, [illegible] Ye, P. Guo, W. Tan, Z. Qing, X.Yang and B. Zhou, *Proc. Natl. Acad. Sci. USA*, 2011, **108**, 3900-3905.

7 A. D. Kent, N. G. Spiropulos and J. M. Heemstra, *Anal. Chem.*, 2013, **85**, 9916-9923.

8 (a) A. K. Sharma and J. M. Heemstra, *J. Am. Chem. Soc.*, 2011, **133**, 12426-12429. (b) M. N. Stojanovic, P. de Prada and D. W. Landry, *J. Am. Chem. Soc.,* 2000, **122**, 11547-11548.

9 (a) R. Yamamoto-Fujita and P. K. R. Kumar, *Anal. Chem.*, 2005, **77**, 5460-5466. (b) C. H. Lu, F. Wang and I. Willner, *Chem. Sci.*, 2012, **3**, 2616-2622.

10 (a) J. Zhang, L. Wang, D. Pan, S. Song, F. Y. C. Boey, H. Zhang and C. Fan, *Small*, 2008, **4**, 1196-1200. (b) X. Zuo, Y. Xiao and K. W. Plaxco, *J. Am. Chem. Soc.*, 2009, **131**, 6944-6945. (c) J. Liu, Y. Liu, X. Yang, K. Wang, Q. Wang, H. Shi and L. Li, *Anal. Chem.*, 2013, **85**, 11121-11128. (d) A. K. Sharma, A. D. Ke[illegible] and J. M. Heemstra, *Anal. Chem.*, 2012, **84**, 6104-6109. (e) C. Wu, L. Yan, C. Wang, H. Lin, C. Wang, X. Chen and C. J. Yan, *Biosens. Bioelectron.*, 2010, **25**, 2232-2237.

11 D. Shangguan, Y. Li, Z. Tang, Z. C. Cao, H. W. Chen, P. Mallikaratchy, K. Sefah, C. J. Yang and W. Tan, *Proc. Natl. Acad. Sci. USA*, 2006, **103**, 11838–11843.

12 D. Shangguan, Z. Cao, L. Meng, P. Mallikaratchy, K. Sefah, H. Wang, Y. Li and W. Tan, *J. Proteome Res.*, 2008, **7**, 2133-2139

13 D. Shangguan, Z. Tang, P. Mallikaratchy, Z. Xiao and W. Tan, *ChemBioChem*, 2007, **8**, 603-606.

14 J. Zhu, T. Nguyen, R. Pei, M. Stojanovic and Q. Lin, *Lab Chip*, 2012, **12**, 3504-3513.

15 (a) S. Nagrath, L. V. Sequist, S. Maheswaran, D. W. Bell, [illegible] Irimia, L. Ulkus, M. R. Smith, E. L. Kwak, S. Digumarthy, [illegible] Muzikansky, P. Ryan, U. J. Balis, R. G. Tompkins, D. A. Haber and M. Toner, *Nature*, 2007, **450**, 1235-1239. (b) W. Sheng, T. Chen, R. Kamath, X. Xiong, W. Tan and Z. H. Fan, *Anal. Chem.*, 2012, **84**, 4199-4206. (c) Z. Ying, W. Yi, A. M. George, A. M. Steinbach, B. E. Phillips, G. Nick, E. S. Gawalt and W. S. Me[illegible]g. *Biomaterials*, 2011, **32**, 249–257. (d) W. Yi, L. Wen, C. Ba[illegible]ia, S. Zhang, M, Bai, J. M. Janjic, G. Nick, E. S. Gawalt and S. [illegible] Wilson. *Acta Biomater*, 2014, **10**, 4759–4767.

16 M. N. Stojanovic, P. D. Prada and D. W. Landry, *J. Am. Chem. Soc.*, 2001, **123**, 4928-4931.